

A light-front wavefunction approach to heavy quark fragmentation in the QGP

Rishi Sharma^{1,*} Ivan Vitev^{1,†} and Ben-Wei Zhang^{1,2‡}

¹ *Los Alamos National Laboratory, Theoretical Division, Los Alamos, NM 87545, USA and*

² *Institute of Particle Physics, Central China Normal University, Wuhan, 430079, China*

We calculate the charm and beauty fragmentation functions in the vacuum using their operator definitions in factorized perturbative QCD and find leading corrections that arise from the structure of the final-state hadrons. In the framework of potential models we demonstrate the existence of open heavy flavor bound states in the QGP in the vicinity of the critical temperature and provide first results for the in-medium modification of the heavy quark distribution and decay probabilities in a co-moving plasma. In an improved perturbative QCD description of heavy flavor dynamics in the thermal medium we combine D and B meson formation and dissociation with parton-level charm and beauty quark quenching to obtain predictions for the heavy meson and non-photonic electron suppression in Cu+Cu and Pb+Pb collisions at RHIC and the LHC, respectively.

PACS numbers: 24.85.+p; 25.75.-q; 12.38.Mh

I. INTRODUCTION

The early production of heavy quarks makes them some of the most important probes of the quark-gluon plasma (QGP) created in ultra-relativistic collisions of heavy nuclei [1]. Precise and direct measurements of the multiplicities and differential distributions of D and B hadrons will soon become available with the vertex detector upgrades at the Relativistic Heavy Ion Collider (RHIC) and at the Large Hadron Collider (LHC). Such experimental advances will allow to quantitatively address the key observable in heavy ion physics - the apparent modification of particle production by energetic partons traversing a region of hot and dense nuclear matter [2, 3, 4] - for heavy quark jets. In the framework of perturbative Quantum Chromo-Dynamics (pQCD), studies in this direction have focused so far exclusively, with varying degree of sophistication, on the kinematic re-distribution of the leading parton or particle energy via radiative and collisional energy loss [5, 6] and, more recently, via meson dissociation in the QGP [7, 8, 9].

It is, therefore, surprising that to date there has been no theoretical evaluation of the modification of the quark distribution (PDF) and fragmentation (FF) functions themselves in the presence of a thermal medium. Heavy flavor provides the ideal testing ground for our first quantitative study of these effects since the lowest lying Fock

state in the light-front wavefunction expansion for D and B mesons [10, 11] can be approximately obtained by boosting the hadron rest-frame solution to the corresponding Dirac equation [12, 13]. Furthermore, potential model calculations can be generalized up to temperatures of order few T_c [14] using lattice QCD input [15]. We carry out this program for open heavy flavor and present results for the D and B meson PDFs and FFs in a co-moving quark-gluon plasma. For the realistic case of out-of-equilibrium fast jet propagation in the thermal medium we compare the relative importance of charm and beauty parton energy loss processes and D and B meson dissociation as a function of transverse momentum. We discuss the prospects of constraining the pQCD theory by upcoming open heavy flavor measurements at RHIC and the LHC.

Our paper is organized as follows: in Section II we present a detailed baseline calculation of charm and beauty quark production, inclusive of the known cold nuclear matter effects, and expose the limitations of the purely partonic approach to their final-state dynamics in the QGP. Derivation of the relation between the parton distribution and decay probabilities of heavy quarks in hadrons and a calculation of the c and b quark PDFs and FFs is given in Section III. In Section IV we evaluate the heavy meson wave-functions in the vacuum and in the vicinity of the QCD phase transition and present numerical results for the corresponding distribution and decay probabilities. A complete calculation that includes D and B meson dissociation and c and b quark quenching, relevant to current and future heavy flavor/non-photonic electron measurements, is given in Section V. Finally, we present our conclusions in Section VI.

*Electronic address: rishi@lanl.gov

†Electronic address: ivitev@lanl.gov

‡Electronic address: bzhang@lanl.gov

II. A TIMELESS LIMIT

To correctly assess the discrepancy between the expected heavy quark quenching and the measured non-photon electron suppression [16, 17] improved treatment of cold nuclear matter effects is necessary. We calculate the charm and beauty quark cross sections per elementary nucleon-nucleon collisions as follows:

$$(N_{\text{bin.}}^{AB})^{-1} \frac{d\sigma_{AB}^{q,g}}{dy d^2\mathbf{p}_T} = K \sum_{abcd} \int dy_d \int d^2\mathbf{k}_a d^2\mathbf{k}_b \frac{f(k_b)f(k_b)}{|J(k_a, k_b)|} \times \frac{\alpha_s(\mu_r)}{2S} |\overline{M}_{ab \rightarrow cd}|^2 \frac{\phi_{a/N}(\frac{\tilde{x}_a}{1-\epsilon_a}, \mu_f) \phi_{b/N}(\frac{\tilde{x}_b}{1-\epsilon_b}, \mu_f)}{\tilde{x}_a \tilde{x}_b}. \quad (1)$$

In Eq. (1) $\mu_r = m_T = (m_{q,g}^2 + p_T^2)^{1/2}$ and the Jacobian $J(k_a, k_b) \propto S$. We have generalized the pQCD collinear factorization approach to heavy flavor production [18, 19] to account for the non-zero parton transverse momentum distribution $f(k_{a,b})$ in the hadron wavefunction with $\langle k_{a,b}^2 \rangle = 0.9 \text{ GeV}^2$. Hence, in p+A and A+A reaction Cronin effect can now be taken into account in the p_T -differential cross sections by including parton k_T broadening from initial-state scattering: $\langle k_{a,b}^2 \rangle_{AB} = \langle k_{a,b}^2 \rangle_{pp} + \langle k_{a,b}^2 \rangle_{IS}$ [20, 21]. These multiple collisions also give rise to radiative energy loss that is sensitive to the quark mass [22] and is implemented in Eq. (1)

as follows: $\tilde{x}_{a,b} \rightarrow \frac{\tilde{x}_{a,b}}{1-\epsilon_{a,b}}$ with $\epsilon_{a,b} = \frac{\Delta E_{a,b}^{\text{rad}}}{E_{a,b}}$ evaluated in the rest frame of the target nucleus. Last but not least, power-suppressed [23] resummed [24, 25] coherent final-state scattering of the struck parton that leads to shadowing in the observed cross sections is included via [18]: $\tilde{x}_a = x_a \left(1 + \frac{\xi_a^2(A^{1/3}-1)}{-t+m_d^2}\right)$, $\tilde{x}_b = x_b \left(1 + \frac{\xi_b^2(A^{1/3}-1)}{-\tilde{u}+m_c^2}\right)$. Our results, reported here, bring the treatment of cold nuclear matter effects for open heavy flavor production on par with their implementation in the study of light hadron and direct photon final states [26]. The numerical values of the quark and gluon mean free paths $\lambda_{q,g}$, the typical transverse momentum squared per unit length $(\mu^2/\lambda)_{q,g}$ and the related scale of power corrections per nucleon $\xi_{a,g}^2$ can also be found in Ref. [26]. Linear dependence of cold nuclear matter effects on the mean nuclear thickness of the interaction region is implicit in our approach.

Next, we turn to the final-state heavy quark dynamics that is governed by the formation times of the plasma [27], τ_0 , and of the hadrons [7],

$$\tau_{\text{form}} \simeq \frac{2z(1-z)E_T}{\mathbf{k}^2 + (1-z)m_h^2 - z(1-z)m_q^2}. \quad (2)$$

During the collision the energy density of the partonic system builds through a short exponential growth [27], which we assume to occur around $\tau_0 = 0.6 \text{ fm}$ and $\tau_0 = 0.3 \text{ fm}$ at RHIC and LHC, respectively, and at $t < \tau_0$ particles are largely unaffected by the medium. Let us first ignore the fact that τ_{form} in Eq. (2) can be smaller than the size of the medium and calculate the ra-

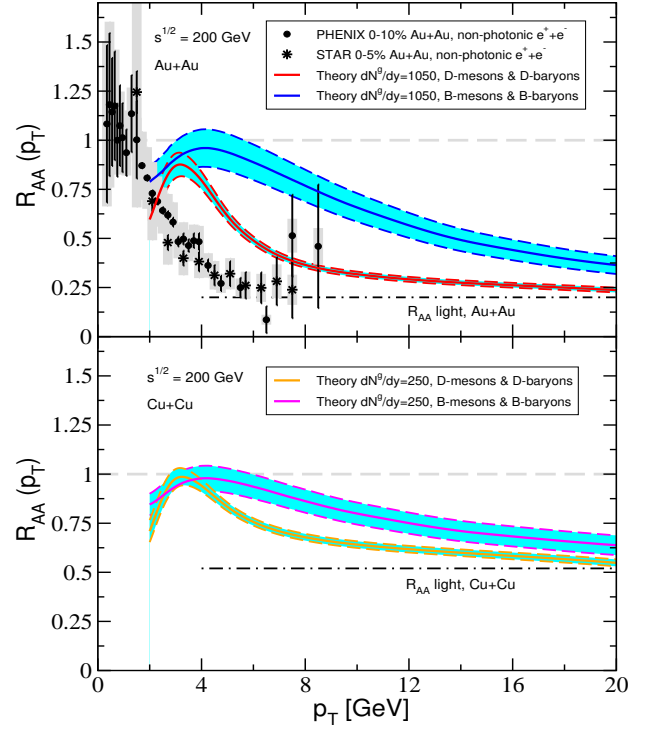


FIG. 1: Perturbative QCD calculation of the suppressed D and B meson production cross sections in central Au+Au (top panel) and Cu+Cu (bottom panel) collisions is compared to the magnitude of light pion quenching at $\sqrt{s_{NN}} = 200 \text{ GeV}$. The effect of parton mass on the cold nuclear matter effects is illustrated via uncertainty bands. Non-photon electron data from PHENIX [16] and STAR [17] is also shown.

diative energy loss for light and heavy partons to first order in opacity following the theoretical approach outlined in [22]. In Ref. [28] a complete and numerically intensive evaluation of jet production, distributed $\propto \frac{dN^{\text{bin.}}}{d^2x_T}$, and propagation through 1+1D expanding QGP, distributed $\propto \frac{dN^{\text{part.}}}{d^2x_T}$ was carried out. We found that the energy loss pattern is determined by the jets originating near the peak of the binary collision density. Therefore, we here focus only on the partons produced at the center of the collision geometry, use a running coupling constant at the radiation vertex and describe the strength of the interactions of the jet with the medium by an effective value $\alpha_s = 0.28 - 0.32$. Any uncertainty associated with higher orders in opacity and peripheral jets will lead to somewhat larger values of α_s .

Having evaluated the probability distribution for the jet fractional energy loss $P(\epsilon)$, $\epsilon = \sum_i \frac{\Delta E_i}{E}$ due to multiple gluon emission, the quenched parton spectrum is readily obtained:

$$\frac{d\sigma_{AB}^{q,g \text{ Quench}}(p_T)}{dy d^2\mathbf{p}_T} = \int_0^1 d\epsilon P(\epsilon) \frac{1}{(1-\epsilon)^2} \frac{d\sigma_{AB}^{q,g}(\frac{p_T}{1-\epsilon})}{dy d^2\mathbf{p}_T}. \quad (3)$$

Hadronization is performed using the appropriate vac-

uum fragmentation functions:

$$\frac{d\sigma_{AB}^h(p_T)}{dyd^2\mathbf{p}_T} = \sum_{q,g} \int_0^1 dz D_{h/q,g}(z, \mu_{fr}) \times \frac{1}{z^2} \frac{d\sigma_{AB}^{q,g} \text{Quench} \left(\frac{p_T}{z} \right)}{dyd^2\mathbf{p}_T}. \quad (4)$$

Schematic representation of the suppression rate $R_{AA}(p_T)$ of π^0 s, or $\frac{1}{2}(\pi^+ + \pi^-)$, in central Au+Au (top panel) and Cu+Cu (bottom panel) reactions, compatible with recent PHENIX [29, 30] and STAR [31] results, is shown in Figure 1. We used gluon rapidity densities $dN^g/dy = 1050$ and $dN^g/dy = 250$, respectively, and the same figure illustrates the attenuation of D and B mesons. It is easy to see that Cronin enhancement plays an important role at intermediate $p_T \sim 4$ GeV and the bands show the sensitivity of cold nuclear matter effects on the parton mass in the range from 0 to m_c, m_b , respectively. At mid-rapidity the effect of high-twist shadowing is small and the uncertainty band is dominated by initial state energy loss. Thus, cold nuclear matter effects amplify the disparity between the light and heavy parton quenching. In contrast, the experimental results on non-photonic electrons [16, 17] $R_{AA}^{\pm} \sim R_{AA}^0$, $p_T > 5$ GeV are in clear contradiction with the minimal quenching of B mesons that give an increasingly important $\geq 50\%$ contribution to non-photonic $e^+ + e^-$ in this region [32]. Meson dissociation, facilitated by a short $\tau_{\text{form}} \propto 1/m_h^2$, naturally leads to attenuation of the beauty cross section as large as that for charm [7].

III. DISTRIBUTION AND FRAGMENTATION FUNCTIONS OF HEAVY QUARKS

Simulations of heavy quark fragmentation and dissociation in the QGP require knowledge of the corresponding parton decay and distribution probabilities. These are related to the wave-functions of their parent or decay hadrons. Proper construction of the non-perturbative lowest order Fock component in the expansion of a hadronic state in a quark and gluon basis appears to be the most important. Higher order components, when generated via perturbative parton splitting, are then guaranteed to have the correct quantum numbers through preservation of all relevant global symmetries in QCD. Furthermore, for heavy mesons the $Q\bar{q}$ or $\bar{Q}q$ provide good representation of the momentum distribution of heavy versus light quarks:

$$|\vec{\mathbf{P}} = 0; J\rangle_h = \int \frac{d^3\vec{\mathbf{q}}}{(2\pi)^3} \frac{M(j)_{s_1 s_2}}{\sqrt{2}} \frac{\delta_{c_1 c_2}}{\sqrt{3}} f(\vec{\mathbf{q}}) \times \sqrt{\frac{E_h}{2E_1 E_2}} a_Q^{\dagger s_1 c_1}(\vec{\mathbf{q}}) b_q^{\dagger s_2 c_2}(-\vec{\mathbf{q}})|0\rangle, \quad (5)$$

where $\vec{\mathbf{q}}$ represents the relative momentum between quarks in the meson rest frame and $f(\vec{\mathbf{q}})$ is the Fourier

transform of the coordinate-space meson wavefunction. $M(j)$ ensure the correct spin structure of pseudoscalar 1S_0 and vector 3S_1 states and proper normalization, $\langle \vec{\mathbf{P}}; J, \lambda | \vec{\mathbf{P}}' J, \lambda' \rangle = 2E_H (2\pi)^3 \delta^3(\vec{\mathbf{P}} - \vec{\mathbf{P}}') \delta_{\lambda\lambda'}$, is provided by having $(2\pi)^{-3} \int d^3\mathbf{q} |f(\mathbf{q})|^2 = 1$.

To evaluate the PDFs and FFs it will be useful to also write the wavefunction in a light-cone form by changing variables from $\vec{\mathbf{P}}$ to $\vec{P}^+ \equiv (P^+, \mathbf{P})$, and $\vec{\mathbf{q}}_i$ to $(x_i P^+, x_i \mathbf{P} + \mathbf{k}_i)$. We follow the correspondence discussed in [33] to obtain,

$$|\vec{P}^+; J\rangle = \int \frac{d^2\mathbf{k}}{(2\pi)^3} \frac{dx}{2\sqrt{x(1-x)}} \frac{M(j)_{s_1 s_2}}{\sqrt{2}} \frac{\delta_{c_1 c_2}}{\sqrt{3}} \psi(x, \mathbf{k}) \times a_Q^{\dagger s_1 c_1}(x\vec{P}^+ + \mathbf{k}) b_q^{\dagger s_2 c_2}((1-x)\vec{P}^+ - \mathbf{k})|0\rangle \quad (6)$$

where \mathbf{k} represents the transverse momentum and x is the large light-front momentum fraction. Conversion between the instant and light-cone forms is facilitated if harmonic oscillator, or Gaussian, approximation is made for the shape of the wavefunction [33], which allows to easily ensure identical transverse width $\langle \mathbf{k}^2 \rangle$ [7].

In the light-cone gauge $A^+ = 0$, the heavy quark distribution function is given by [34]:

$$\phi_{Q/h}(x) = \int \frac{dy^-}{2\pi} e^{-ixP^+y^-} \times \langle P^+ | \bar{\psi}_Q(y^-, \mathbf{0}) \frac{\gamma^+}{2} \psi_Q(0, \mathbf{0}) | P^+ \rangle, \quad (7)$$

where ψ_Q is the heavy quark field operator and the average over the hadron spin/polarization states is implicit. For both the pseudoscalar and the vector cases after straightforward evaluation at tree level we find:

$$\phi_{Q/h}(x) = \frac{1}{2(2\pi)^3} \int dx_Q d^2\mathbf{k} |\psi(x_Q, \mathbf{k})|^2 \delta(x_Q - x). \quad (8)$$

In contrast, the tree level calculation of fragmentation of the heavy quark into hadron h , defined as [34]:

$$D_{h/Q}(z) = z \int \frac{dy^-}{2\pi} e^{i\frac{p^+}{z}y^-} \frac{1}{3} \text{Tr}_{color} \frac{1}{2} \text{Tr}_{Dirac} \frac{\gamma^+}{2} \times \langle 0 | \psi(y^-, \mathbf{0}) a_h^{\dagger}(P^+) a_h(P^+) \bar{\psi}(0, \mathbf{0}) | 0 \rangle, \quad (9)$$

shows that since $z = p_h^+/p_Q^+ \leq 1$ and the momentum fraction of the heavy quark in the meson $x_Q \leq 1$, only exclusive $z = x_Q = 1$ hadroproduction is possible. Such processes are exponentially suppressed and in the region of interest $D_{h/Q}(z < 1) \equiv 0$.

The first non-trivial contribution to $D_{h/Q}(z)$ comes from the Feynman diagram shown in Fig. 2. Our approach is similar to the one outlined in [35, 36] but in the calculation we retain $\vec{\mathbf{q}}$, the $Q\bar{q}$ relative momentum distribution, in the matrix element. This will allow us to calculate the lowest order correction in \mathbf{q} to $D(z)$. We do this calculation for the pseudoscalar mesons first. After converting the integral over the transverse momentum of

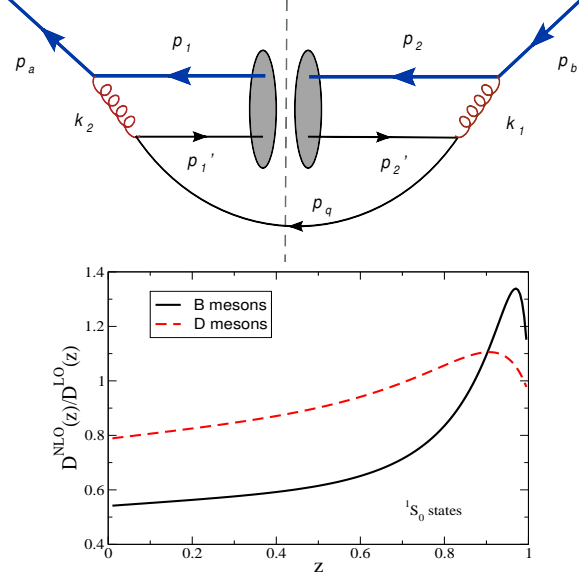


FIG. 2: Top panel: perturbative QCD calculation of heavy quark fragmentation matched to the lowest lying Fock state in the heavy meson wavefunction. Bottom panel: ratio of the first order corrected value $D^{(1)}(z)$ to the zeroth order term $D^{(0)}(z)$ for heavy quark fragmentation in pseudoscalar final states.

the outgoing free light parton \mathbf{p}_q into an integral over the virtuality of the heavy quark we obtain:

$$D_{h/Q}(z) = \int \frac{dx_1 d^2 \mathbf{k}_1}{(2\pi)^3 2\sqrt{x_1(1-x_1)}} \frac{dx_2 d^2 \mathbf{k}_2}{(2\pi)^3 2\sqrt{x_2(1-x_2)}} \frac{M(j)_{s_1 s'_1}}{\sqrt{2}} \frac{M(j)_{s_2 s'_2}}{\sqrt{2}} \int ds \theta \left(s - \frac{m_h^2}{z} - \frac{m_q^2}{1-z} \right) \frac{\alpha_s^2 C_F^2}{3} \frac{\text{Tr} \left[\gamma^+ \frac{i}{\gamma \cdot p_a - m_Q} \gamma^\mu u_{s_1}(p_1) \bar{v}_{s'_1}(p'_1) \gamma^\nu (\gamma \cdot p_q + m_q) \gamma^\sigma v_{s'_2}(p'_2) \bar{u}_{s_2}(p_2) \gamma^\lambda \frac{i}{\gamma \cdot p_b - m_q} \Pi_{\mu\nu}(p_a - p_q) \Pi_{\sigma\lambda}(p_b - p_q) \right]}{\text{Tr}[\gamma^+(\gamma \cdot p)]}, \quad (10)$$

where $\Pi_{\mu\nu}(p_a - p_q)$ is the gluon propagator. The full result of the above expression is very complex and requires the use of packages for Dirac algebra manipulation [37]. The calculation is facilitated by considering the mean distribution of the large momentum between in the quark-antiquark pair, which in the absence of relative $\vec{\mathbf{q}}$ in Eq. (5) yields $r = m_q/(m_Q + m_q)$, $1 - r$. In practice, for D and B mesons with the exception of B_c this assumption leads to decay probabilities that are peaked at values of z that are too large when compared to experimental data. Hence, r is usually treated as a phenomenological parameter. If the hadron wavefunctions, Eqs. (5) and (6), are

known, then:

$$r = \frac{\sqrt{m_q^2 + \langle \mathbf{k}^2 \rangle}}{\sqrt{m_q^2 + \langle \mathbf{k}^2 \rangle} + \sqrt{m_Q^2 + \langle \mathbf{k}^2 \rangle}}, \quad (11)$$

can be obtained from the calculated $\langle \mathbf{k}^2 \rangle = \langle \mathbf{q}^2 \rangle$. We will use Eq. (11) to evaluate r both in the vacuum and at non-zero temperature. The internal structure of hadrons is also reflected in the fragmentation functions through the explicit \mathbf{k}_1, x_1 and \mathbf{k}_2, x_2 dependence in Eq (10). We have checked that if this dependence is neglected, equivalent to taking the $\vec{\mathbf{q}} = 0$, we recover the functional form for $D_{h/Q}(z)$ obtained in [36]. If we keep the next-to-leading term in $\vec{\mathbf{q}}_1$ and $\vec{\mathbf{q}}_2$ in the limit of large $p_a^+(p_b^+)$ and carry out the numerical integration over the relative parton momenta inside the hadron [38] we find the corrections to the charm and beauty decay probabilities in 1S_0 states that are shown in the lower panel of Fig. (2). The fragmentation functions themselves are normalized to unity and the corrections obtained this way are relatively small. We defer the discussion of the corrections to the vacuum fragmentation to a more detailed study [38].

IV. THE FATE OF HEAVY MESONS BELOW AND ABOVE T_c

Potential models have been quite useful in studying the non-perturbative aspects of QCD. In particular, for quarkonia one can put the potential model on firm grounds by using an effective field theory (NRQCD) [39]. More generally, heavy-light mesons like the D and the B and their excited states at zero temperature have been studied in detail [12, 13] by treating the light \bar{q} as a Dirac particle moving in a confining potential set up by the heavy quark Q . In this section we investigate the bound-state solutions for D and B mesons at non-zero temperatures which will allow us to calculate the PDFs and FFs for quarks/mesons in a co-moving thermal medium, as discussed above.

Lattice QCD results for the free energy of a system at temperature T containing two infinitely heavy quarks separated by a distance r [15] have been used to extract the static potential between these quarks:

$$V(r) = \begin{cases} -\frac{\alpha}{r} + \sigma r, & r < r_{med}(T) \\ -\frac{\alpha_1(T) \exp(-\mu(T)r)}{r} + \sigma r_{med}(T), & r > r_{med}(T) \end{cases}. \quad (12)$$

Here, $r_{med}(T)$ signifies the temperature-dependent distance scale at which the medium breaks off the linear confining potential, $\alpha_1(T)$ represents the effective coupling at a given temperature, and $\mu(T)$ is the Debye screening mass. A suitable interpolation is used to smooth out the sharpness in the potential at $r = r_{med}$. This potential, has been employed previously to study the fate of heavy-heavy bound states in the QGP formed at temperatures above T_c [14, 40].

The typical parameters used in Eq. (12) are $\alpha = 0.445$, $\alpha_1(T) = \frac{1}{3\pi}g^2(2\pi T)$, $\mu(T) = 1.417\sqrt{1 + \frac{N_f}{6}g(2\pi T)T}$, with renormalized coupling constant g calculated at two loops, and $r_{med}(T) = 0.4\frac{T_c}{T}$ in fm. The strength of the confining potential $\sigma = 0.224 \text{ GeV}^2$ and $T_c = 192 \text{ MeV}$. The value of σ is $\approx 5\%$ larger than in [40] and we take $M_c = 1.34 \text{ GeV}$ and $M_b = 4.79 \text{ GeV}$. The presence of bound states like charmonia and bottomonia can be explored by solving the non-relativistic Schrödinger equation for the heavy quarks in the presence of the potential Eq. (12). We find that J/ψ exists up to about $2T_c$ though they have a binding energy, quite sensitive to the precise value of σ , much less than the temperature. The Υ disappears at much higher temperatures but its binding energy becomes smaller than T near $1.5T_c$.

To investigate the existence of heavy-light mesons in the QGP by solving the Dirac equation we first need to separate the scalar $V_s(r)$ from the vector $V_v(r)$ part of the potential, Eq. (12), as described for $T = 0$ in [12, 13]. In Eq. (12) the term proportional to σ , which in the absence of a medium would be a confining linear potential, is scalar. The Coulomb part is naturally interpreted as the zeroth component of a vector potential. For $T > T_c$ $r_{med}(T)$, $\alpha_1(T)$ and $\mu(T)$ are as discussed above. For $T < T_c$, instead of using the perturbative expression for $g(2\pi T)$, we take $g = 2.05$ to be independent of temperature. Finally, $r_{med} = \min(0.4\frac{T_c}{T}, 1.1) \text{ fm}$, where 1.1 fm is the typical string breaking scale [40].

The eigenfunctions of the spherically symmetric Dirac Hamiltonian, $-i\gamma^0\gamma^i\partial_i + V_v(r) + \gamma^0(m + V_s(r))$, can be written as [12, 13, 41, 42],

$$\psi(\mathbf{r}) = \frac{1}{r} \begin{pmatrix} G(r) \\ i\sigma \cdot \hat{\mathbf{r}}F(r) \end{pmatrix} \mathcal{Y}_{jl}^{j_3}, \quad (13)$$

where $\mathcal{Y}_{jl}^{j_3}$ are angular functions that are obtained by angular momentum addition of $s = \frac{1}{2}$ to l to give j . The energy eigenequations for the radial wavefunctions $F(r)$ and $G(r)$ that we need to solve are as follows:

$$\begin{cases} F'(r) - \frac{\kappa}{r}F(r) = (-E + V_v(r) + m + V_s(r))G(r) \\ G'(r) + \frac{\kappa}{r}G(r) = (E - V_v(r) + m + V_s(r))F(r), \end{cases} \quad (14)$$

T	$T(\text{GeV})$	$E_b(\text{GeV})$	$\sqrt{\langle r^2 \rangle}(\text{GeV})^{-1}$
0	0	0.730	2.374
$0.2T_c$	0.038	0.733	2.361
$0.4T_c$	0.077	0.611	2.351
$0.6T_c$	0.115	0.256	2.540
$0.8T_c$	0.154	0.098	3.202
$1.0T_c$	0.211	0.043	3.980
$1.2T_c$	0.230	0.031	4.917
$1.4T_c$	0.269	0.017	6.402

TABLE I: Properties of the bound D and B meson states taking the effective light quark mass to be $m(T)/\sqrt{2}$. These persist up to temperatures $\approx 1.5T_c$.

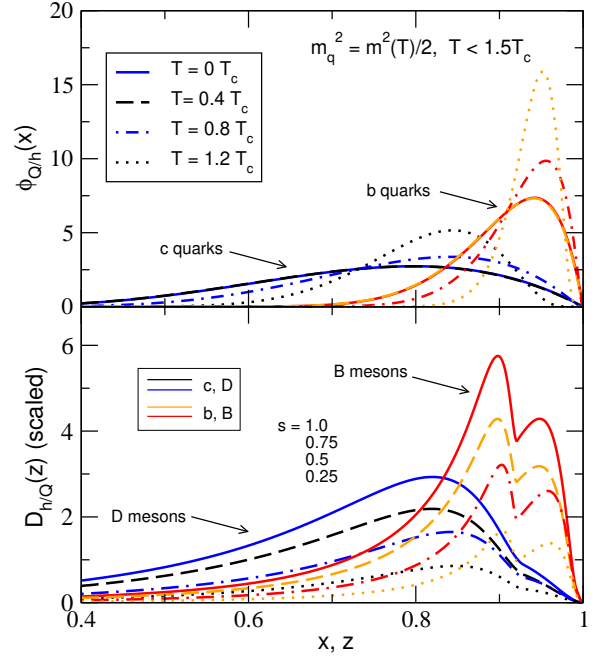


FIG. 3: The evolution of FFs $\phi_{Q/H}(x)$ (top panel) and the PDFs $D_{H/Q}(z)$ (bottom panel) with T . Blue/black lines refer to charm while red/orange lines refer to beauty. A scale factor s has been used to better separate the decay probabilities.

where $\kappa = \pm(j + 1/2)$. For the lowest energy states that we are interested in, $j = 1/2$ and $\kappa = -1$. We solve numerically the system Eq. (14) using the “shooting method”.

Since the heavy-light mesons are larger in size when compared to quarkonia, it is natural to expect that they will be affected more severely by color screening. Indeed, for a light current quark mass of about 0.005 GeV , we don’t find even very weakly bound states for $T > T_c$. However, this conclusion is quite sensitive to the parameters chosen above. For example, by simply changing r_{med} from $0.4\frac{T_c}{T} \text{ fm}$ to $0.45\frac{T_c}{T} \text{ fm}$ [14] we find bound states up to $\sim 1.2T_c$, albeit with binding energies E_b about 50 times smaller than T . A quark moving in the QGP will have an effective thermal mass larger than its bare mass m_q . For $T > T_c$ perturbative calculations give $m(T) = \sqrt{\frac{C_F}{4}(g(2\pi T))^2 + m_q^2}$. For $T < T_c$ this form is not valid so we simply interpolate the perturbative value above T_c to the bare mass at $T = 0$. One would expect the effective mass of a quark moving under the influence of a potential in the thermal medium to lie somewhere between m_q and $m(T)$. For example, results obtained by solving the Dirac equation for the light quark mass taken to be $m(T)/\sqrt{2}$ are given in Table I. We remark that the very small rise in the binding energy that can be seen in Table I as we increase the temperature from $T = 0$ to $0.2T_c$ is an artifact of the interpolation we have used for the thermal mass below T_c and is not numerically significant to affect our results. The use of light

quark mass equal to $m(T)$ gives bound-state solutions with weak binding energies up to about $T \approx 1.9T_c$. We also establish the existence of D and B meson states well above the phase transition temperature for constituent light quark masses and/or for the “maximum confining potential” compatible with lattice data: all the way up to $\sim 2T_c$ for $m_q = m(T)/\sqrt{2}$ and $\sim 3T_c$ for $m_q = m(T)$.

The bound-state wavefunctions, calculated at temperatures $T = 0T_c, 0.4T_c, 0.8T_c, 1.2T_c$ are employed to evaluate the PDFs and FFs of heavy quarks in a co-moving thermal medium from Eqs. (8), (10) and (11) and our results are presented in Fig. 3. The distribution functions $\phi_{Q/H}(x)$ become narrower in x as we increase the temperature, which is intuitively expected because the wavefunctions become broader in position space. In contrast the peak position and width of the decay probabilities are determined by the boost parameter r . These remain nearly constant because the decrease in the mean transverse momentum squared is largely compensated by the growth in the thermal mass. Hence, we have used an arbitrary scale factor s to better separate the curves in the bottom panel of Fig. 3. To summarize, as a rule we find that D and B meson bound-state solutions persist above T_c . Their small binding energy and large radius, however, will greatly facilitate their subsequent dissolution in the presence of interactions.

V. APPLICATION TO HEAVY MESON PRODUCTION IN HEAVY ION COLLISIONS

Heavy flavor dynamics in the thermal medium critically depends on the time scales involved in the underlying reaction. Two of these timescales, τ_0 and L_{QGP} , can be related to the nuclear geometry, the QGP expansion, and the properties of bulk particle production [28]. They signify the onset and disappearance of in-medium effects and determine, in relation to the formation time Eq. (2), whether the suppression of the observed cross section arises predominantly at the hadronic ($\tau_{\text{form}} \ll L_{QGP}$) or partonic ($\tau_{\text{form}} \geq L_{QGP}$) levels. As discussed in the previous section, the dissociation of D and B mesons in the vicinity of T_c can be facilitated by their small binding energy, or, equivalently, their broad wavefunction in coordinate space. Whether such thermal effects take place in practice, however, depends on the time they need to develop. We can roughly estimate this time by boosting the expanded size of the hadron, $\approx 2\sqrt{\langle r^2 \rangle}$ from Table I, by the γ factor. When compared to τ_{form} , which is determined by the virtuality in the parton decay process, this time is large and suggests that the fragmentation component of the heavy meson dynamics in heavy ion collisions may not be affected by the QGP. In what follows we will study this “instant wavefunction limit” in detail. Whether accelerated initial D and B meson dissociation in conjunction with extended subsequent quark interactions in the medium (suppressed fragmentation) can phenomenologically describe the non-photonic $e^+ + e^-$

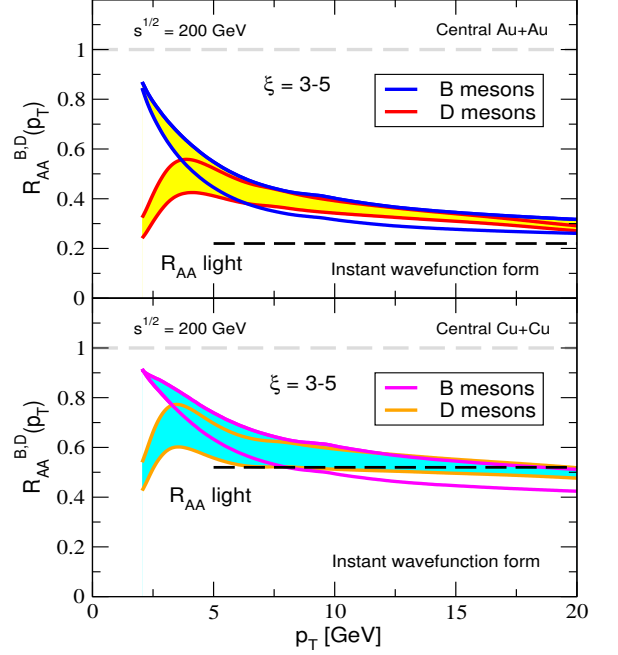


FIG. 4: Suppression of D and B hadron production from meson dissociation and heavy quark quenching in central Au+Au (top panel) and Cu+Cu collisions (bottom panel) at $\sqrt{s_{NN}} = 200$ GeV at RHIC.

quenching is an investigation that goes beyond the scope of our current paper [38].

The concurrent processes of c and b quark fragmentation and D and B meson dissociation are described by the following set of rate equations [7]:

$$\begin{aligned} \partial_t f^Q(p_T, t) = & -\frac{1}{\langle \tau_{\text{form}}(p_T, t) \rangle} f^Q(p_T, t) \\ & + \frac{1}{\langle \tau_{\text{diss}}(p_T/\bar{x}, t) \rangle} \int_0^1 dx \frac{1}{x^2} \phi_{Q/H}(x) f^H(p_T/x, t), \quad (15) \end{aligned}$$

$$\begin{aligned} \partial_t f^H(p_T, t) = & -\frac{1}{\langle \tau_{\text{diss}}(p_T, t) \rangle} f^H(p_T, t) \\ & + \frac{1}{\langle \tau_{\text{form}}(p_T/\bar{z}, t) \rangle} \int_0^1 dz \frac{1}{z^2} D_{H/Q}(z) f^Q(p_T/z, t). \quad (16) \end{aligned}$$

Note that the reason for which the asymptotic $t \rightarrow \infty$ solution will exhibit suppression of the cross sections is that both fragmentation and dissociation processes emulate energy loss by shifting the quarks/hadrons to lower momenta. At present, there is no reliable way of incorporating the fluctuations in partonic energy loss in rate or transport equations. Therefore, we include the early-time heavy quark inelastic scattering effects approximately as a quenched initial condition:

$$\begin{cases} f^Q(p_T, t) = \frac{d\sigma^Q(t)}{dyd^2p_T}, & f^Q(p_T, 0) = \frac{d\sigma^{Q, \text{Quench}}}{dyd^2p_T}, \\ f^H(p_T, t) = \frac{d\sigma^H(t)}{dyd^2p_T}, & f^H(p_T, 0) = 0. \end{cases}$$

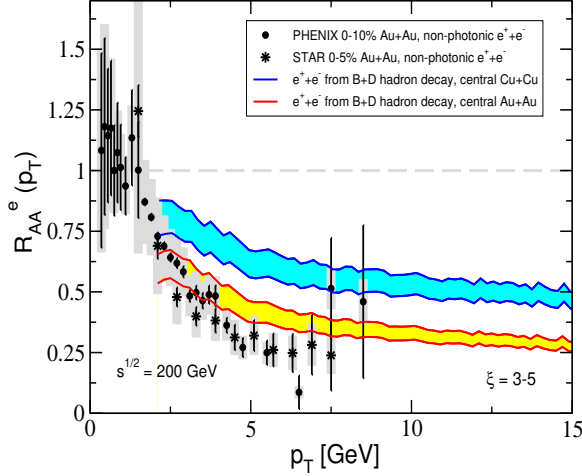


FIG. 5: Nuclear modification for the single non-photonic electrons in central Au+Au and Cu+Cu collisions at RHIC. Data is from the PHENIX [16] and STAR [17] collaborations.

Here, the attenuated partonic spectrum $\frac{d\sigma^{Q, \text{Quench}}}{dy d^2p_T}$ is calculated differentially versus p_T as in Eq. (3) over a time period $\tau_p = \tau_{\text{form}}(1 + (L_{QGP} - \tau_{\text{form}})/L_{QGP})$ if $\tau_{\text{form}} < L_{QGP}$. In the limit of $\tau_{\text{form}} \gg L_{QGP}$ our calculation reduces to the results given in Fig. (1). This approach should be valid as long as the dissociation rate is not very large.

In our numerical calculations we use the same initial soft gluon rapidity density dN^g/dy as in the simulations of π^0 quenching. The corresponding suppression of open heavy flavor in $\sqrt{s_{NN}} = 200$ GeV central Au+Au and Cu+Cu collisions at RHIC is shown in the top and bottom panels of Fig. 4, respectively. For D mesons the Cronin effect is clearly visible around $p_T \sim 4$ GeV and this is a notable difference from our previous study [7] where initial-state k_T diffusion was not included. For B mesons the change in heavy quark velocity β_Q , which controls the $Q\bar{Q}$ ($\bar{Q}Q$) broadening $\propto \beta_Q \frac{\mu_0^2}{\chi_0^2} \xi \ln \frac{\tau}{\tau_0}$ and dissociation, results in the characteristic rapid decrease in $R_{AA}^B(p_T)$ in this part of phase space. In both gold and copper reactions at RHIC the suppression $R_{AA}^B \approx R_{AA}^D$ for $p_T > 5$ GeV and these approach the quenching of light hadrons for $p_T > 10$ GeV. It should be noted that while for the D mesons we observe a transition from collisional dissociation to partonic energy loss in the studied kinematic domain, for B meson at RHIC the competing hadronic processes, Eqs. (15) and (16), still play the dominant role.

Our theoretical results, presented in Fig. 4, are most relevant to the future vertex detector upgrades at RHIC that will ensure direct and separate measurements of the D and B mesons. These new experimental data will then allow to pinpoint the mechanisms of heavy flavor suppression in the QGP. Indirect studies of D and B meson attenuation are currently carried out through the semi-

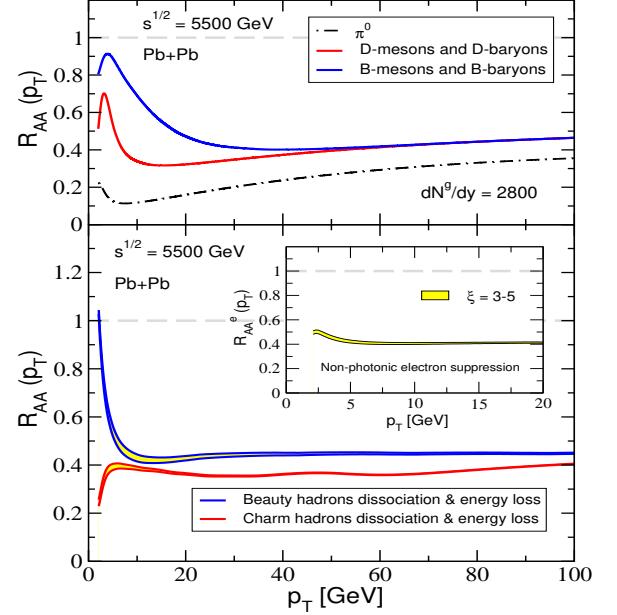


FIG. 6: Suppression of D and B meson production in central Pb+Pb collisions at $\sqrt{s_{NN}} = 5500$ GeV at LHC in two different scenarios. The top panel shows the quenching of heavy hadrons only due to partonic energy loss. The bottom panel gives R_{AA} for D s and B s with partonic energy loss as well as collisional dissociation of heavy meson. Insert shows the corresponding attenuation of non-photonic electrons in a limited p_T range.

leptonic decays of the charm and beauty hadrons. We use the PYTHIA event generator [44] to simulate the full kinematics of these Dalitz decays in p+p and A+A reactions. The nuclear modification ratio $R_{AA}^e(p_T)$ of inclusive non-photonic electrons is presented in Fig. 5 for $\sqrt{s_{NN}} = 200$ GeV collisions at RHIC. Predictions for central Cu+Cu collisions are also shown for comparison to upcoming STAR data. We remark that the Cronin effect included in our study changes the absolute scale of the differential heavy quark cross section at intermediate p_T . Consequently, to obtain a good description of the non-photonic $e^+ + e^-$ quenching results from PHENIX [16] and STAR [17] we use $\xi = 3 - 5$, approximately 50% larger than in our previous study [7] but still compatible with the enhancement of the parton broadening that comes from the power-law momentum transfer tails of the in-medium Moliere scattering.

Results for the suppression of open heavy flavor final states in central Pb+Pb collisions at $\sqrt{s_{NN}} = 5500$ GeV at the LHC in a medium of soft gluon rapidity density $dN^g/dy = 2800$ are presented in Fig. 6. The top panel illustrates the effect of partonic energy loss with $R_{AA}^B(p_T) = R_{AA}^D(p_T)$ for $p_T \geq 40$ GeV. D and B meson quenching approaches the suppression level of light hadrons only at very high transverse momentum due to the significant gluon fragmentation component to

pion production in this kinematic region. The bottom panel shows the attenuation of open heavy flavor when we include collisional dissociation in the medium. The most important feature of our results, when compared to traditional jet quenching studies, is that at the LHC $R_{AA}^B(p_T) \approx R_{AA}^D(p_T)$ at a much lower $p_T \simeq 10$ GeV. The nuclear modification factor of non-photonic electrons is also shown for completeness in the insert of Fig. 6. By comparing the top and bottom panels of Fig. 6 we conclude that only experiments at the LHC will have the transverse momentum coverage to fully explore heavy flavor dynamics in the QGP. We finally remark that, at present, we don't consider the small difference in the suppression of D and B mesons physically significant. This question requires further investigation [38].

VI. CONCLUSIONS

Detailed theoretical studies have shown that partonic energy loss of heavy quarks in the hot QGP [6] cannot explain the large suppression of non-photonic electrons observed by the PHENIX [16] and STAR [17] collaborations in central Au+Au collisions at $\sqrt{s_{NN}} = 200$ GeV per nucleon pair. This discrepancy can naturally be resolved if collisional dissociation of heavy mesons that tend to form inside the QGP is taken into account [7]. In this Letter we reported first results from an approach that attempts to combine charm and beauty quark quenching with D and B meson inelastic breakup processes with the goal of describing open heavy flavor production in nucleus-nucleus collisions over the full p_T range that will be experimentally accessible at RHIC and the LHC. The treatment of cold nuclear matter effects for massive final states was brought on par with that for pions and photons [26] and the Cronin enhancement at transverse momenta ~ 4 GeV was found to be the most important. To put studies of heavy meson formation and dissociation in the plasma [7, 8] on firmer theoretical ground we investigated in the framework of potential models [14] the existence of such bound states in the vicinity of T_c .

We found that while the temperature at which D and B mesons cease to form depends on the details of the in-medium quark-antiquark potential and the light quark mass, as a rule bound states survive well above T_c . Using the light-front description of hadrons [11] and the operator definitions of distribution and decay probabilities from factorized perturbative QCD [34] we calculated the charm and beauty PDFs and FFs in a co-moving plasma.

In the instant wavefunction approximation, relevant to an out-of-equilibrium jet propagation through the medium when the timescale for the onset of thermal effects exceeds τ_{form} , we evaluated the D and B meson cross section suppression from partonic and hadronic interactions in the QGP. We found that for $p_T > 5$ GeV at RHIC and $p_T > 10$ GeV at the LHC $R_{AA}^B(p_T) \approx R_{AA}^D(p_T)$ and the transverse momentum dependence of this attenuation is weak. In our study meson dissociation played the dominant role up to $p_T \sim 10$ GeV for open charm and up to $p_T \sim 30$ GeV for open beauty hadrons. To obtain a good description of the non-photonic electron suppression in Au+Au collisions at RHIC after the inclusion of Cronin enhancement [20] approximately 50% larger collisional broadening [21] that leads to the meson breakup was required. Predictions were given for the D and B hadron and the corresponding non-photonic electron quenching in Cu+Cu and Pb+Pb collisions at RHIC and the LHC, respectively, that will very soon be confronted by experimental data. We conclude by emphasizing that for a comprehensive and definitive study that can disentangle the medium effects on b quarks/ B mesons, in particular, not only the enhanced cross sections but also the extended p_T reach of LHC experiments will play a critical role.

Acknowledgments

This research is supported by the US Department of Energy, Office of Science, under Contract No. DE-AC52-06NA25396 and in part by the LDRD program at LANL, the NNSF of China and the MOE of China under Project No. IRT0624.

-
- [1] A. D. Frawley, T. Ullrich and R. Vogt, Phys. Rept. **462**, 125 (2008); references therein.
 - [2] D. d'Enterria, arXiv:0902.2011 [nucl-ex].
 - [3] G. David, arXiv:0903.0336 [nucl-ex].
 - [4] M. Gyulassy, I. Vitev, X. N. Wang and B. W. Zhang, arXiv:nucl-th/0302077.
 - [5] B. W. Zhang, E. Wang and X. N. Wang, Phys. Rev. Lett. **93**, 072301 (2004).
 - [6] S. Wicks, W. Horowitz, M. Djordjevic and M. Gyulassy, Nucl. Phys. A **783**, 493 (2007).
 - [7] A. Adil and I. Vitev, Phys. Lett. B **649**, 139 (2007).
 - [8] F. Dominguez and B. Wu, Nucl. Phys. A **818**, 246 (2009).
 - [9] F. Dominguez, C. Marquet and B. Wu, arXiv:0812.3878 [nucl-th].
 - [10] M. Burkardt, Adv. Nucl. Phys. **23**, 1 (1996).
 - [11] S. J. Brodsky, H. C. Pauli and S. S. Pinsky, Phys. Rept. **301**, 299 (1998).
 - [12] M. Avila, Phys. Rev. D **49**, 309 (1994).
 - [13] M. A. Avila, Mod. Phys. Lett. A **14** 2059 (1999).
 - [14] A. Mocsy and P. Petreczky, Phys. Rev. D **77**, 014501 (2008).
 - [15] O. Kaczmarek and F. Zantow, Phys. Rev. D **71**, 114510 (2005).
 - [16] A. Adare *et al.* [PHENIX Collaboration], Phys. Rev. Lett. **98**, 172301 (2007).
 - [17] B. I. Abelev *et al.* [STAR Collaboration], Phys. Rev. Lett.

- 98**, 192301 (2007)
- [18] I. Vitev, T. Goldman, M. B. Johnson and J. W. Qiu, Phys. Rev. D **74**, 054010 (2006).
 - [19] F. I. Olness, R. J. Scalise and W. K. Tung, Phys. Rev. D **59**, 014506 (1999).
 - [20] A. Accardi, arXiv:hep-ph/0212148.; references therein.
 - [21] I. Vitev, Phys. Lett. B **562**, 36 (2003).
 - [22] I. Vitev, Phys. Rev. C **75**, 064906 (2007).
 - [23] J. W. Qiu and G. Sterman, Int. J. Mod. Phys. E **12**, 149 (2003).
 - [24] J. W. Qiu and I. Vitev, Phys. Rev. Lett. **93**, 262301 (2004).
 - [25] J. W. Qiu and I. Vitev, Phys. Lett. B **632**, 507 (2006).
 - [26] I. Vitev and B. W. Zhang, Phys. Lett. B **669**, 337 (2008).
 - [27] A. Dumitru, Y. Nara and M. Strickland, Phys. Rev. D **75**, 025016 (2007).
 - [28] I. Vitev, S. Wicks and B. W. Zhang, JHEP **0811**, 093 (2008)
 - [29] A. Adare *et al.* [PHENIX Collaboration], Phys. Rev. Lett. **101**, 162301 (2008).
 - [30] A. Adare *et al.* [PHENIX Collaboration], Phys. Rev. C **77**, 064907 (2008)
 - [31] B. I. Abelev *et al.* [STAR Collaboration], Phys. Lett. B **655**, 104 (2007).
 - [32] G. Wang [STAR Collaboration], J. Phys. G: Nucl. Part. Phys. **35** 104107 (2008).
 - [33] B. Q. Ma, Z. Phys. A **345**, 321 (1993).
 - [34] J. C. Collins and D. E. Soper, Nucl. Phys. B **194**, 445 (1982).
 - [35] J. P. Ma, Phys. Lett. B **332**, 398 (1994).
 - [36] E. Braaten, K. M. Cheung, S. Fleming and T. C. Yuan, Phys. Rev. D **51**, 4819 (1995).
 - [37] R. Mertig, M. Bohm and A. Denner, Comput. Phys. Commun. **64**, 345 (1991).
 - [38] R. Sharma, I. Vitev and B. W. Zhang, in preparation.
 - [39] N. Brambilla, A. Pineda, J. Soto and A. Vairo, Rev. Mod. Phys. **77**, 1423 (2005).
 - [40] A. Mocsy and P. Petreczky, Phys. Rev. Lett. **99**, 211602 (2007).
 - [41] J. J. Sakurai, *Advanced Quantum Mechanics*, First ISE reprint, Addison-Wesley Publishing Company Inc. (1999)
 - [42] W. Greiner, *Relativistic Quantum Mechanics*, Berlin, Springer-Verlag (1990).
 - [43] K. M. Cheung and T. C. Yuan, Phys. Rev. D **53**, 1232 (1996).
 - [44] T. Sjostrand, S. Mrenna and P. Skands, JHEP **0605**, 026 (2006).